Wildfire risk management across diverse bioregions in a changing climate

Tristan Campbell, S. Don Bradshaw, Kingsley W. Dixon & Philip Zylstra

View supplementary material

Published online: 05 Sep 2022.

Submit your article to this journal

View related articles

View Crossmark data

Taylor & Francis
Taylor & Francis Group

Wildfire risk management across diverse bioregions in a changing climate

Tristan Campbell[a] (iD), S. Don Bradshaw[b] (iD), Kingsley W. Dixon[a] (iD) and Philip Zylstra[a] (iD)

[a]School of Molecular and Life Sciences, Curtin University, Bentley, Australia; [b]School of Biological Sciences, University of Western Australia, Nedlands, Australia

ABSTRACT

Wildfire risk-management needs to consider interrelated factors that influence fire regimes, including changing climate and sometimes conflicting stakeholder priorities. With wildfires increasing in size and intensity over recent decades, wildfire risk management is becoming more important and more complex. For southwest Australia, wildfire risk-management is predicated on a longitudinal study of the relationship between prescribed burns and wildfires from 1953–2004 over a subset of this biodiverse region. Our study replicates the methodology of the longitudinal study, applying it to the wider region and extending the analysis to 2021. We found the extrapolation of the longitudinal study's findings to the wider region invalid, as was extrapolation beyond 2004. In particular, the area of prescribed burns generally had negligible influence on wildfire area. However, more spatially complex fire history was strongly correlated with lower probability of large wildfires (independent of area burned). This highlights the limitation of extrapolating wildfire risk-management policies to areas of differing vegetation and/or climate, including changing climate over time. The potential of indigenous-led practices for wildfire risk and biodiversity conservation, particularly for areas with high spatial variability, is apparent as is the need for alternative strategies to prescribed burning as the primary tool in wildfire-risk mitigation.

Introduction

Wildfires are increasingly resulting in adverse impacts around the world (Jones et al. 2022). Of the four primary processes that influence wildfire behaviour: (biomass/necromass or fuel volume, ability of biomass to burn, weather and ignition source (Bradstock 2010), biomass/necromass reduction is typically the focus of efforts to manage wildfire risk (Jenkins et al. 2020). With both the geographic extent and

---

Supplemental data for this article can be accessed online at https://doi.org/10.1080/19475705.2022.2119891

duration of fire weather increasing globally over the past four decades due to climate change (Jolly et al. 2015) there is a heightened focus on managing wildfire risk through biomass/necromass reduction (Burrows and McCaw 2013).

Fire regimes, defined as the frequency, seasonality and intensity of fires across an area (Krebs et al. 2010), are strongly influenced by climate and vegetation (Archibald et al. 2013). Altered fire regimes can create feedbacks that may have positive or negative impacts on flammability and fire risk, and are affected by both natural and artificial ignitions (Zylstra et al. 2022). The degree and direction of feedbacks are highly dependent again on the climate and vegetation characteristics of the area in question.

Effective wildfire risk management requires consideration of these complex, interrelated factors, along with the public perception of wildfire risk against other values, such as protection of property and lives, biodiversity conservation, climate change and government agency effectiveness (Bardsley et al. 2018). This often results in conflicting perceptions and priorities amongst stakeholders (Driscoll et al. 2010; Bentley et al. 2017).

For the global threatened biodiversity hotspot of southwest Australia (Myers et al. 2000), government policy for wildfire risk management by the Department of Biodiversity, Conservation and Attractions (DBCA) is founded on the longitudinal study of fire data by (Boer et al. 2009) from 1953 to 2003, which is used to design an annual target of 200,000 ha of prescribed burns over a 2.5 million ha section of the public forest estate (Burrows and McCaw 2013), divided into three Land Management Zones (LMZs). Our study replicates the methodology of Boer et al. (2009), deploying the same methodology to assess the applicability of the findings from Boer et al. (2009) over the same southwest region of Australia where wildfire risk management policy is based on these findings. Our aim is to determine whether the extrapolation of Boer et al. (2009) to the broader southwest region provides a relevant basis for the wildfire risk management policy, and whether this remains valid with the addition of a further 17 years' of fire history data through to 2021.

Materials and methods

Study area

Of the four recognised Interim Biogeographic Regions of Australia (IBRA) (DAWE 2020) over which the wildfire risk management policy is applied, the longitudinal study by Boer et al. (2009) covers an area encompassing subsections of two regions (see Figure 1 and Table 1). Archibald et al. (2013) defines two fire regimes for the study area over recent decades, with the majority of the area being classed as an 'intermediate-cool-small' wildfire regime (three-month fire season, 12-year fire return interval, less than 1% burnt annually and maximum fire size less than 9 km^2) and the western-most section of the Warren region classed as a 'rare-cool-small' wildfire regime (one-month fire season, > 50 year fire return interval, less than 0.5% burnt annually and maximum fire size less than 4 km^2).

The current wildfire risk management policy is applied across a much wider range of average annual weather conditions and vegetation classes than the region studied by Boer et al. (2009) (see Figure 2). Climatic trends of decreasing rainfall and
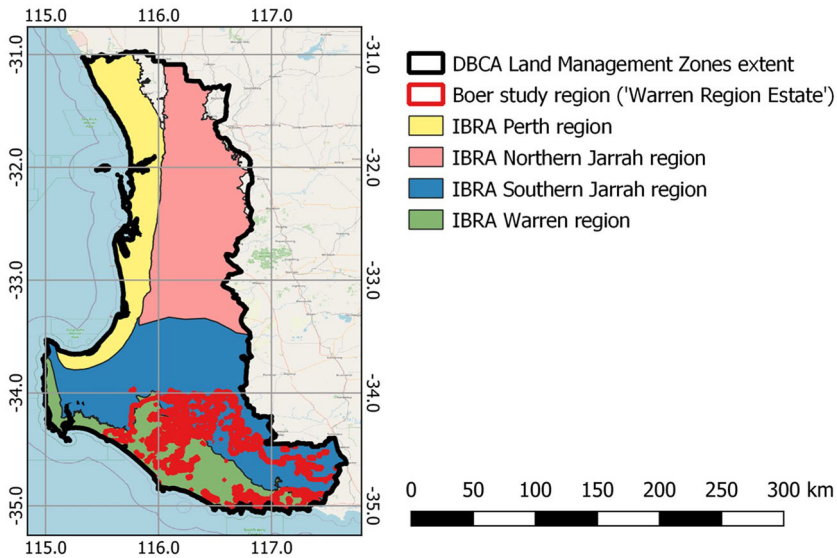
Figure 1. Geographic regions used for this study. Basemap from OpenStreetMap Contributors (2021).
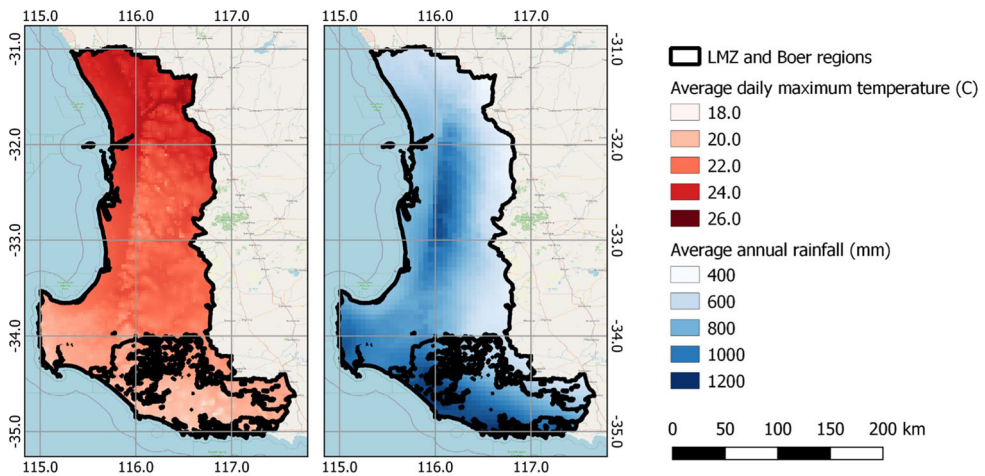
Figure 2. Range of average daily maximum temperatures and total annual rainfall for the study area. Weather data from *Maps and gridded spatial data. Bureau of Meteorology* [accessed 2022 Jan 15]. http://www.bom.gov.au/climate/data-services/maps.shtml. Basemap from OpenStreetMap Contributors (2021).

increasing temperature have continued from the longitudinal study period to the present day (see Figure 3) and are projected to continue under climate change models (Andrys et al. 2017). As a result, trends in fire behaviour are likely to have altered in the 17 years from the conclusion of the longitudinal study period, and therefore influenced the relationship between prescribed burn regimes and wildfires on a landscape scale.
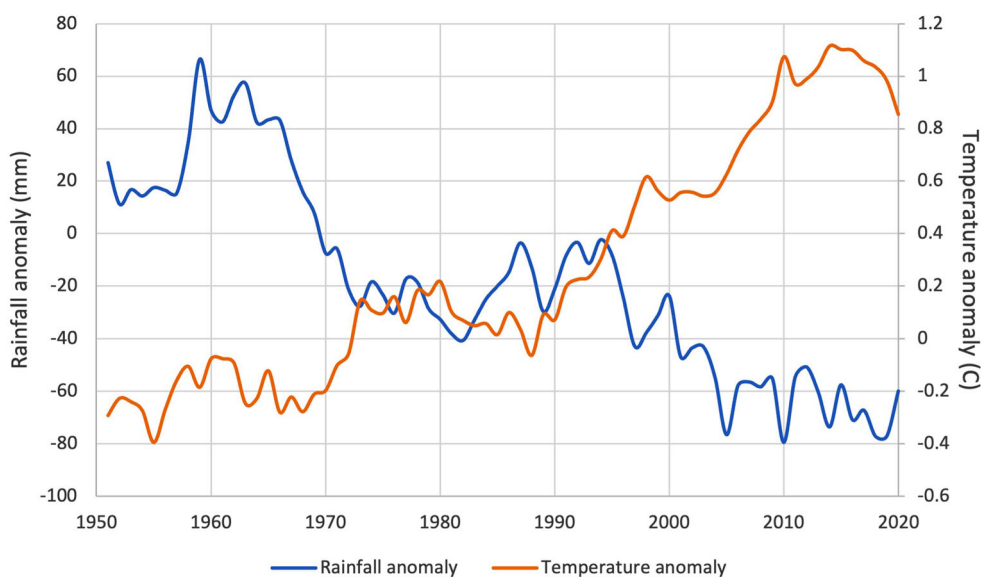
Figure 3. 10-year running mean trends in rainfall and temperature anomalies for south-west Australia. Data from *Climate change – trends and extremes. Bureau of Meteorology* [accessed 2022 Jan 15]. http://www.bom.gov.au/climate/change/#tabs=Tracker.

Data sources

Fire history data were sourced from the December 2021 update of the same dataset used by Boer et al. (2009) (DBCA 2021a), and are derived from a combination of historical records and digital spatial data as well as remote sensing for recent decades. Note that the 'fire year' of this dataset is from 1st July to 30th June the following year (i.e. a 'fire year' of 2005 is from 01/07/2005 to 30/06/2006). From here on, all references to year are 'fire year', hence the data ranged from 1953 to 2020.

Information extracted from this dataset consists of polygons of mapped fire events with key attributes including the date of fire, fire type (Prescribed Burn, Wildfire) and the area of the fire in hectares. The DBCA Fire History dataset (DBCA_060) was cropped to the geographic extent of DBCA's Prescribed Burns—Land Management Zones (LMZs) dataset (DBCA 2021b) which is a close approximation to the South West Fire Management Area (FMA) defined by Howard et al. (2020).

It is recognised that the accuracy of the fire history dataset has improved over time, especially with the increasing improvements in the temporal, spatial and spectral resolution of satellite data in the past few decades used by DBCA to map the extents of wildfires in particular. There is therefore a focus on the changes in large wildfire events over time, as these represent the largest risk events, account for the vast majority of the area burnt by wildfire over the study period and are likely to be the most accurately recorded wildfires in the older portions of the fire history dataset. This focus may reduce some of the issues encountered when comparing fire extents delineated by different approaches, as presented by Skakun et al. (2021) and is consistent with Wang et al. (2021), who found that the annual total extent of wildfires is often best predicted by the size of the largest individual wildfire.

Mean window	Year	0	1	2	3	4	5	6	7	8	9	10
WF 1-1	PB	■										
	WF		■									
WF 1-2	PB	■										
	WF		■	■								
WF 1-3	PB	■										
	WF		■	■	■							
WF 1-4	PB	■										
	WF		■	■	■	■						
WF 1-5	PB	■										
	WF		■	■	■	■	■					
WF 1-6	PB	■										
	WF		■	■	■	■	■	■				
WF 1-7	PB	■										
	WF		■	■	■	■	■	■	■			
WF 1-8	PB	■										
	WF		■	■	■	■	■	■	■	■		
WF 1-9	PB	■										
	WF		■	■	■	■	■	■	■	■	■	
WF 1-10	PB	■										
	WF		■	■	■	■	■	■	■	■	■	■
Boer et. al.(2009)	PB	■	■	■	■	■	■					
	WF	■	■	■	■	■	■					

Figure 4. Graphical representation of time averaging windows used to calculate regressions between mean extents of prescribed burns and wildfires.

Statistical analysis

Initial analysis assessed the length of time that the annual extent of prescribed burns in one year correlated with reduced extent of wildfires in following years. To find this, we replicated the approach used by Boer et al. (2009) using logarithmic-linear quantile regression performed using the 'statsmodels' module for Python 3 (Seabold and Perktold 2010). This was performed for annual wildfire extents of time lags of up to 10 years from a given annual prescribed burn extent, for both the 1953–2003 time period used by Boer et al, and for the full 1953–2020 dataset.

Implicit in this approach is the assumption that wildfire extent relates to the fuel reduction effect of preceding prescribed burns, but not preceding wildfires. Although this assumption does not reflect the true area of each region burnt in years preceding wildfires, we replicated it, for consistency, as part of the approach of Boer et al. (2009).

One of the core findings of Boer et al. (2009) was the measurement of 'leverage' (Loehle 2004), which is the inverse gradient of the relationship of wildfire extent to prescribed fire extent. To determine leverage, we analysed the annual extent of prescribed burns *versus* the mean annual extent of wildfires using averaging windows from one to up to ten years after the given prescribed burn. Logarithmic-linear regressions were used for consistency with the quantile regression and linear regressions to calculate the leverage of prescribed burns (linear gradient).

In replicating the approach of Boer et al. (2009), we noted that the regression was performed on the mean extent of prescribed burns and wildfires in concurrent six-year averaging windows (Figure 4). For example, the mean for annual prescribed burn extent for 1961 to 1966 was correlated against the mean annual wildfire extent for 1961 to 1966. Therefore, changes in wildfire extent are partially attributed to

prescribed burns carried out *after* the wildfires had occurred. This approach also means that offsets of zero to five years were assessed, not up to six years.

As this was an unexpected finding, the results were verified by digitizing the annual prescribed burn and wildfire fire extent data in Boer et al. (2009) and independently plotting and performing logarithmic-linear and linear regression models on the concurrent six-year running average windows of the prescribed burn and wildfire data. These results were compared with the plots and regression models in Boer et al. (2009) and found to be consistent. Despite this anomaly, we replicated this analysis for consistency, referring to it as the PB6vsWF6 period.

Influence of spatial patterns of fire history

For multi-parameter spatial pattern analysis, we assessed the relationship between area burnt by wildfires and changing fire management, drought index and fuel age spatial patterns using the 'explained deviance' parameter from Generalised Additive Models (GAMs). GAMs were generated using pyGAM (Serven and Brummitt 2018), from the annual extent of wildfires mapped in the DBCA_060 dataset with Keetch-Byram Drought Index (KBDI) and output from time since fire spatial pattern analysis.

We calculated daily cumulative time-series KBDI from 01/07/1953 to 30/06/2021 on a 5 km grid using gridded daily maximum temperature and daily rainfall data taken from the Bureau of Meteorology's gridded historical data (Bureau of Meteorology 2021). This has been shown to be the most spatially accurate source of weather data for the study region (Campbell and Fearns 2022). The lack of daily wind speed data across the time range of the study prevented the calculation of other fire danger indices such as the Forest Fire Danger Index (FFDI), which is consistent with Boer et al. (2009). For each fire year in each region, we calculated the median of all daily gridded KBDI points.

The time since fire spatial pattern considers the spatial arrangement of the fire history through measures such as the average size of fire ages patches, how connected patches of more recent or longer time since fire are, and the complexity of individual patches. Spatial pattern analysis was performed on the total fire extent for each year (prescribed burns plus wildfires), transformed into a 100 m x 100 m gridded raster file. The stack of fire extent rasters for the 6 years preceding each year were used to classify each pixel of the layer for each year as comprising either up to six years since fire (= <6TSF) or more than six years since fire (>6TSF), to use the same classification of 'old' and 'young' fuels as Boer et al. (2009). The same five spatial metrics as Boer et al. (2009) were calculated in FRAGSTATS (McGarigal et al. 2012) for each year of analysis for each bioregion and the overall study region. These were:

1. The percentage of the landscape of each time since fire class (PLAND)
2. The number of patches of each time since fire class (NP)
3. The mean area of each time since fire class (AREA_MN)
4. The mean perimeter-area ratio for each time since fire class (PARA)

5. The 'connectedness' of the time since fire class patches, with a threshold distance of 200 m (CONNECT)

To replicate GAM process in Boer et al. (2009), GAMs for each region and time period were also created for the pairwise combination of year (as a proxy for changing prescribed burning protocols and fire-fighting technology) and KBDI. The residual errors from these GAMs were then used as the input to create GAMs for individual and three-factor input models for all time since fire spatial pattern metrics from FRAGSTATS. After modelling every 3-factor combination of the patch metrics as well as each patch metric individually this resulted in 129 GAMs for each time period and region. Again, the 'explained deviance' parameter was used to compare GAM efficacies.

Large wildfire probability

The year and size of each recorded wildfire were used to assess the probability of occurrence of fire sizes (Probability Density Function (PDF)) for each year using the gaussian kernel density estimation function in 'SciPy' module for Python 3 (Virtanen et al. 2020). The resulting PDF was normalised by the highest number of occurrences of fires for each fire size annually, with the final PDF showing the relative likelihood of a fire of a given size for each year from 1953–2020. The mean probability of large wildfires (>1,000 ha) was calculated for each year and qualitatively compared with long-term patterns of prescribed burning extents and quantitatively with the geospatial patch analysis of recent fire history from FRAGSTATS.

Results

Overall temporal trends in fire extent

The annual extent burnt by prescribed burns and wildfires from 1953 to 2020 for each region is shown in Figure 5. The broad inverse relationship between annual prescribed burn extent and wildfire extent described by Boer et al. (2009) is apparent for the Boer region up to 2003. This qualitative relationship between annual extents of prescribed burns and wildfire up to 2003 is also visible for the Warren region and the LMZ, but not in the other three IBRA regions (Southern Jarrah, Northern Jarrah and Perth regions).

When more recent data from 2003–2020 are considered, this relationship between prescribed burn and wildfire extents disappears across all regions. The annual prescribed burn extent for most regions increased slightly from 2003–2020 but with different impacts on wildfire extent. Wildfire extent in the Southern Jarrah region decreased (continuing the trend from prior to 2003) and the Northern Jarrah, LMZ and Boer regions showed no change in the average annual wildfire extent. The Warren region had a decrease in average annual prescribed burn extent after 2003 and no change in average annual wildfire extent. The Perth region had a positive correlation between prescribed burn and average annual wildfire extents after 2003, with wildfire extents increasing with increasing sizes of prescribed burning.
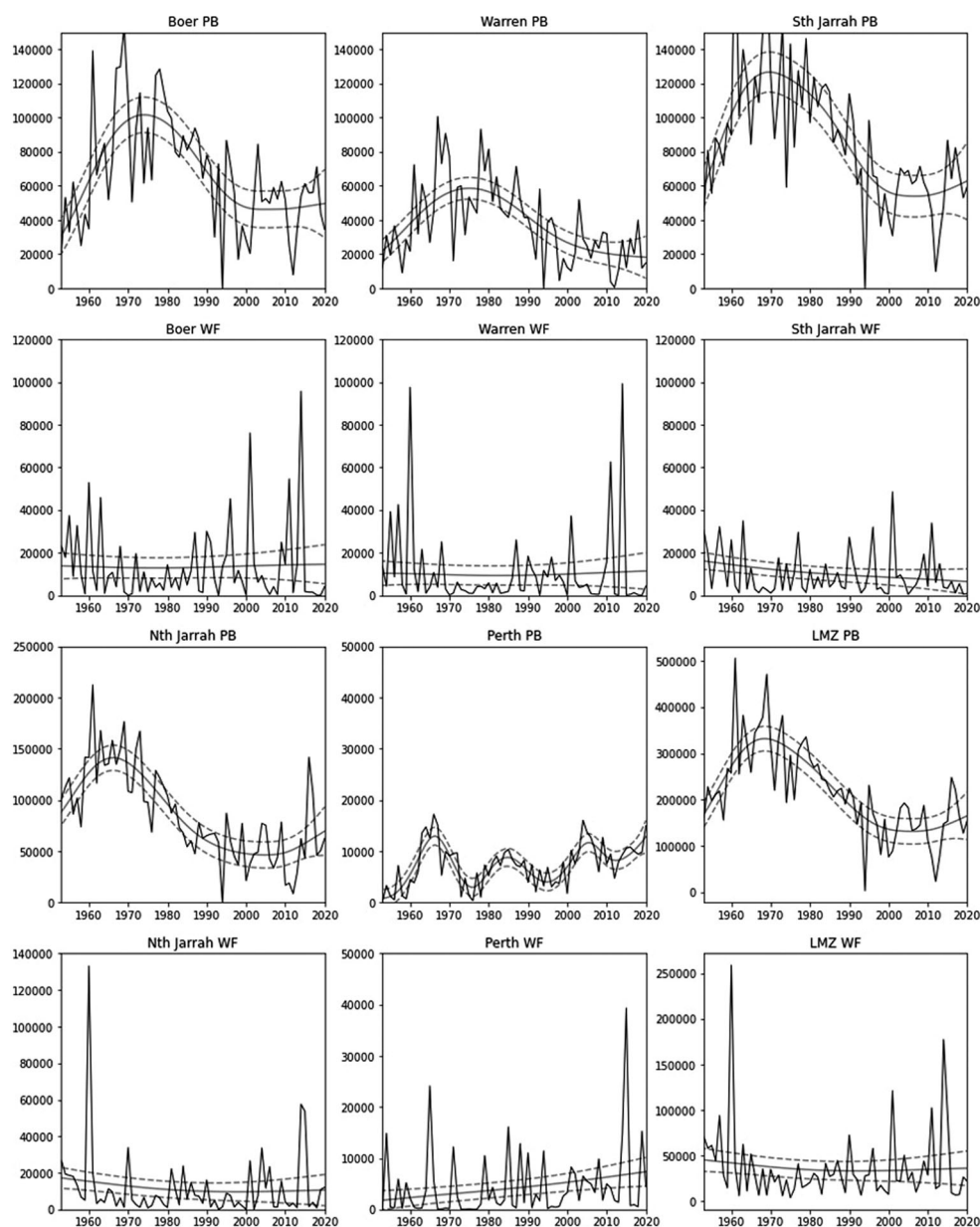
Figure 5. Area burnt by prescribed burn and wildfire for each study region from 1953–2020. Smooth solid lines are linear GAM models, with 95% confidence intervals shown as dashed lines.

Statistical analysis

Quantile regression analysis by Boer et al. (2009) from lag times of zero to eight years found significant negative quantile coefficients for annual wildfire extents with lags of one to four years and six years from annual prescribed burn extents. Boer et al. (2009) deemed the inverse relationship between prescribed burns and wildfires to be significant for the period over which there was a minimum of one significant negative

Quartile	0 years	1 year	2 years	3 years	4 years	5 years	6 years	7 years	8 years
0.05	NO	YES	YES	YES	NO	NO	NO	NO	NO
0.25	NO	YES	NO	YES	NO	NO	NO	NO	NO
0.50	NO	YES	NO	YES	NO	NO	YES	NO	NO
0.75	NO	NO	NO	NO	NO	NO	NO	NO	NO
0.95	NO	YES	YES	NO	YES	NO	NO	NO	NO
>=1 significant negative quartile?	NO	YES	YES	YES	YES	NO	YES	NO	NO

←————————————— DEEMED SIGNIFICANT ————————————→ ←— NOT
          INVERSE RELATIONSHIP   SIGNIFICANT →

Figure 6. Graphical representation of significant inverse relationship is determined for years since prescribed burn. Data are summarised from Appendix S1 of Boer et al. (2009).

quantile regression over a two-year period, concluding that there was a significant negative relationship between the annual extents of prescribed burns and wildfires for up to six years following prescribed burns. This is represented graphically in Figure 6. Note that this is not an assessment of the relationship for any individual fires but an average on a landscape scale.

While the quantile regression results are provided in full in the supplementary material, Table 2 below summarises these data into the period over which there is deemed to be a significant relationship between prescribed burn and wildfire extents as per the definition above. A similar period was found for the Boer region from 1953–2003 as by Boer et al. (2009) of seven years compared to six years. A six-year period was found for the Warren region for both the 1953–2003 and 1953–2020 datasets.

Beyond these three examples, the quantile regression results are markedly different from Boer et al. (2009). This includes the Boer region with data through to 2020, which maintained a significant inverse relationship for greater than 10 years. The LMZ region as a whole had a significant inverse relationship for greater than 10 years over both dataset year ranges. The Southern Jarrah region only had a significant inverse relationship for up to one year and the Northern Jarrah region had none. The Perth region had a zero year period from 1953–2003 but a two year period from 1953–2020, however this was a significant positive relationship rather than negative.

The logarithmic-linear regression Coefficient of Determination (R^2) and linear regression slopes are provided in Table 3. Taking the Boer region from 1953–2003 and the 'PB6vsWF6' window as the benchmark, no other region or data period achieved the same R^2 of 0.70. The next closest R^2 value was 0.39, for the Boer region from 1953–2020. While this is still a significant relationship ($p < 0.001$), it represents a marked drop in correlation. When R^2 is calculated over different windows for mean annual wildfire extent, the correlations are likewise lower (including for the Boer region from 1953–2003). Therefore, no region, data time set or averaging window meets the benchmark R^2 value.

The linear gradient results in Table 3 do show three circumstances where the benchmark of the Boer region from 1953–2003 of −0.20 is met or exceeded (Boer region from 1953–2003 and both datasets from the Warren region) albeit with lower R^2 values. For the remainder of the PB6vsWF6 regressions, the gradients are lower with negative gradients all being less than −0.05. The Perth region has positive

Table 1. Descriptions of IBRA sub-regions.

IBRA sub-region	Description
Warren 75 distinct vegetation complexes	Dissected undulating country of the Leeuwin Complex and Albany Orogen with loamy soils supporting **Karri forests**, laterites supporting **Jarrah-Marri forest**, leached sandy soils in depressions and plains supporting **paperbark/sedge swamps** and Holocene marine dunes with ***Agonis flexuosa* woodlands**.
Jarrah Forest 152 distinct vegetation complexes	Duricrusted plateau of Yilgarn Craton characterised by **Jarrah-Marri forest** on laterite gravels and, in the eastern part, by **Marri-Wandoo woodlands** on clayey soils. Alluvial and alluvial deposits support ***Agonis* shrublands**. In areas of Mesozoic sediments, **Jarrah forests occur in a mosaic with a variety of species-rich shrublands**.
Perth 40 distinct vegetation complexes	Low lying coastal plain, **mainly covered with woodlands**. It is **dominated by Banksia or Tuart** on sandy soils, ***Allocasurina obesa*** on outwash plains and paperbark in swampy areas. In the east, the plain rises to duricrusted Mesozoic sediments dominated by **Jarrah woodland**.

Major vegetation complexes are highlighted in bold.

Table 2. Length of time deemed to have a significant relationship between prescribed annual extent of prescribed burns and wildfires in following years from logarithmic-linear quantile regression.

Region	1953–2003	1953–2020
Boer	7 years	>10 years
Warren	6 years	6 years
Southern Jarrah	1 year	1 year
Northern Jarrah	0 years	0 years
Perth	0 years	2 years[a]
LMZ	>10 years	>10 years

[a]Significant positive rather than inverse relationship.

gradients of greater than 0.30, showing a significant positive correlation between prescribed burn and wildfire extents. As per the R^2 analysis, the gradients for all wildfire averaging windows out to 10 years are lower than the benchmark. For the 1953–2020 period, significant correlations were found for the Warren and LMZ regions when average wildfire extents over 10 years were averaged and the Southern Jarrah region over 9 and 10 years (all $p < 0.05$). However, the gradient of these significant correlations are much lower than Boer et al. (2009) (−0.06 and −0.02 for the Warren and LMZ regions and 0.004 for the Southern Jarrah region over 9 and 10 years). Therefore even where there is a significant correlation between prescribed burn extent and mean wildfire extent over subsequent years, the 'leverage' benefit is negligible compared with Boer et al. (2009)'s leverage of −0.24 over six years.

Influence of spatial patterns of fire history

The patch metric GAM model generated by Boer et al. (2009) from the residual wildfire extent after year and KBDI accounted for 64% of the deviation in annual wildfire extents. We digitised the GAM input data in Boer et al. (2009) and the residual GAM for the most important patch metric (connectedness of patches with greater than six years' time since fire) are shown in Figure 7, resulting in a similar explained deviance of 47% (slightly lower as other patch metrics were not added to generate a 3-factor

Table 3. Results of regression analysis of annual extents of prescribed burning versus wildfires over various time windows.

Region	Period	PB6 vsWF6	WF1	WF2	WF3	WF4	WF5	WF6	WF7	WF8	WF9	WF10
Boer	1953–2003	−0.20 (0.70)***	−0.12 (0.02) N.S.	−0.13 (0.22)***	−0.13 (0.30)***	−0.12 (0.33)***	−0.10 (0.29)***	−0.08 (0.24)***	−0.08 (0.24)***	−0.08 (0.27)***	−0.07 (0.28)***	−0.07 (0.31)***
Boer	1953–2020	−0.21 (0.39)***	−0.13 (0.01) N.S.	−0.14 (0.02) N.S.	−0.14 (0.02) N.S.	−0.12 (0.00) N.S.	−0.10 (0.00) N.S.	−0.08 (0.00) N.S.	−0.08 (0.00) N.S.	−0.06 (0.00) N.S.	−0.05 (0.00) N.S.	−0.04 (0.00) N.S.
Warren	1953–2003	−0.26 (0.34)***	−0.11 (0.00) N.S.	−0.17 (0.18) **	−0.17 (0.27)***	−0.15 (0.26)***	−0.13 (0.23)***	−0.12 (0.22)***	−0.12 (0.22)***	−0.11 (0.20) **	−0.10 (0.21)***	−0.10 (0.24)***
Warren	1953–2020	−0.24 (0.24)***	−0.11 (0.00) N.S.	−0.17 (0.00) N.S.	−0.18 (0.00) N.S.	−0.15 (0.00) N.S.	−0.13 (0.00) N.S.	−0.12 (0.00) N.S.	−0.11 (0.00) N.S.	−0.09 (0.02) N.S.	−0.07 (0.04) N.S.	−0.06 (0.07) *
Southern Jarrah	1953–2003	−0.05 (0.20) **	−0.06 (0.00) N.S.	−0.04 (0.01) N.S.	−0.05 (0.06) N.S.	−0.04 (0.07) N.S.	−0.03 (0.09) *	−0.03 (0.07) N.S.	−0.03 (0.14) *	−0.03 (0.13) *	−0.03 (0.17) **	−0.03 (0.27)***
Southern Jarrah	1953–2020	−0.03 (0.07) *	−0.03 (0.00) N.S.	−0.02 (0.00) N.S.	−0.02 (0.00) N.S.	−0.02 (0.00) N.S.	−0.01 (0.01) N.S.	−0.01 (0.01) N.S.	−0.01 (0.02) N.S.	0.00 (0.04) N.S.	0.00 (0.07) *	0.00 (0.09) *
Northern Jarrah	1953–2003	0.09 (0.17) *	0.07 (0.03) N.S.	0.03 (0.01) N.S.	0.01 (0.00) N.S.	0.00 (0.00) N.S.	0.01 (0.00) N.S.	0.01 (0.00) N.S.	0.00 (0.00) N.S.	0.00 (0.00) N.S.	0.00 (0.00) N.S.	0.00 (0.00) N.S.
Northern Jarrah	1953–2020	0.05 (0.03) N.S.	0.03 (0.01) N.S.	0.00 (0.01) N.S.	−0.01 (0.01) N.S.	−0.02 (0.00) N.S.	−0.02 (0.00) N.S.	−0.01 (0.00) N.S.	−0.01 (0.00) N.S.	−0.01 (0.01) N.S.	0.01 (0.03) N.S.	0.01 (0.06) N.S.
Perth	1953–2003	0.32 (0.28)***	0.20 (0.01) N.S.	0.22 (0.01) N.S.	0.16 (0.00) N.S.	0.10 (0.00) N.S.	0.08 (0.00) N.S.	0.05 (0.00) N.S.	0.02 (0.00) N.S.	0.02 (0.00) N.S.	0.00 (0.00) N.S.	−0.04 (0.04) N.S.
Perth	1953–2020	0.46 (0.37)***	0.28 (0.04) N.S.	0.24 (0.01) N.S.	0.15 (0.00) N.S.	0.12 (0.00) N.S.	0.09 (0.01) N.S.	0.07 (0.02) N.S.	0.02 (0.03) N.S.	0.02 (0.03) N.S.	0.04 (0.02) N.S.	0.01 (0.03) N.S.
LMZ	1953–2003	0.01 (0.00) N.S.	−0.04 (0.01) N.S.	−0.05 (0.02) N.S.	−0.06 (0.08) *	−0.06 (0.10) *	−0.05 (0.12) *	−0.05 (0.13) *	−0.05 (0.16) *	−0.05 (0.18) **	−0.05 (0.19) **	−0.05 (0.25)***
LMZ	1953–2020	−0.04 (0.07) *	−0.07 (0.00) N.S.	−0.08 (0.00) N.S.	−0.08 (0.00) N.S.	−0.07 (0.00) N.S.	−0.06 (0.00) N.S.	−0.05 (0.00) N.S.	−0.05 (0.00) N.S.	−0.04 (0.02) N.S.	−0.02 (0.0) N.S.	−0.02 (0.08) *

Values show the gradient with R^2 in brackets.

N.S. Not significant.

***$p < 0.001$, **$p < 0.01$, *$p < 0.05$.
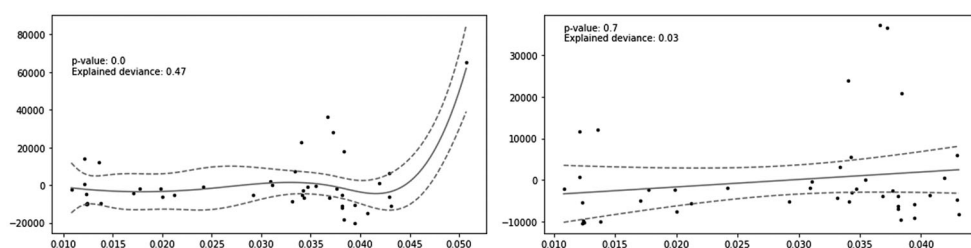
Figure 7. Residual GAM models of 'old fuel' patch connectedness from digitised figures in Boer et al. (2009). Left is full data, right is with the individual significant datapoint/outlier removed.

residual model) which validates the consistency of the statistical methodologies between Boer et al. (2009) and this study. Boer et al. (2009) noted that the primary reason for the high explained deviance was the influence of a single data point with a connectedness of ~0.50. With this datapoint removed (right plot in Figure 7), the significant increasing wildfire extent up to connectedness values of 0.44 stated by Boer et al. (2009) is not apparent.

Residual GAMs generated from the contemporary fire dataset for the same patch metrics had explained deviances of less than 10% in all bar the Northern Jarrah region from 1953–2020 (which had an explained deviance of 27% primarily due to a single datapoint similar to Figure 7) as summarised in Table 4. Residual GAM plots for 1953–2020 are provided in Appendix 1 with a full set of GAM plots in the supplementary material.

Taking the best performing GAM for each region, rather than relying on optimum patch metrics stated by Boer et al. (2009), the Northern Jarrah GAM explained more than 70% of the variation in annual wildfire extents for both time periods. Of the three input factors, both GAMs are primarily influenced by the number of >6TSF patches and connectedness of = <6TSF patches.

Inspecting the residual GAM plots in Appendix 1 for the Northern Jarrah region reveals that the high explained deviance for the number of >6TSF patches is primarily due to overfitting a polynomial curve to one data point and the high explained deviance connectedness of = <6TSF patches primarily due to overfitting to a single high residual value at high connectedness. This implies that highly connected = <6TSF patches positively correlate to larger annual wildfire extents. Removing these patch metrics from the options, the highest explained deviances for GAMs become 0.08 and 0.35 for the 1953 to 2003 and 1953 to 2020 time periods respectively. Therefore the spatial patterns of >6TSF and = <6TSF patches do not explain the majority of the variation in annual wildfire extents.

Large wildfire probability

The fire size probability distribution analysis for both prescribed burns and wildfires for the Boer and Perth regions from 1953 to 2020 is provided in Figure 8, with all regions provided in for this time period in Appendix 2 and all regions for both time periods in the supplementary material. All forest regions (including the overall LMZ region) have similar probability distributions to the Boer region for large fires (1,000

Table 4. Summary of GAM explained deviance results.

Period	GAM	Boer	Warren	Southern Jarrah	Northern Jarrah	Perth	LMZ
1959–2003	Year + KBDI	0.18	0.58	0.03	0.44	0.01	0.44
	Connectedness + perimeter:area ratio + Percentage area	0.04	0.01	0.02	0.03	0.06	0.02
	Best performing	0.07	0.05	0.05	0.75 (0.08)	0.20	0.06
1959–2020	Year + KBDI	0.03	0.05	0.05	0.12	0.04	0.11
	Connectedness + perimeter:area ratio + percentage area	0.06	0.06	0.02	0.27	0.05	0.06
	Best performing	0.07	0.10	0.08	0.74 (0.35)	0.14	0.12

Bracketed values show deviances after the removal of a single outlier datapoints.

to 10,000 ha) to very large fires (>10,000 ha), with large fires significantly more likely to occur before 1960, and very large fires both before 1960 and between ~2000–2015. Large fires were significantly less likely to occur after ~2016 and very large fires significantly less likely to occur between ~1970–1980 and, in most cases, after ~2018.

With the annual extent of prescribed burns reaching a maximum in the late 1970s for all forest regions, this significant increase in very large fires commences approximately 25 years after the maximum PB period and the decrease occurs approximately 40 years after the commencement of the lower PB period. This is in line with the findings of Zylstra et al. (2022).

In the predominantly woodland Perth region, the temporal variations in probability of large wildfires and annual extent of prescribed burning are markedly different from the other regions (Figures 5 and 8), with a cycle of higher prescribed burn extents in the mid 1960s, 1980s and 2000s with lower extents in the mid 1970s, 1990s and 2010s. The last few years of data (up to 2020) show a marked increase in PB extent trending upwards. Against this pattern, wildfires of all sizes were least likely to occur in the mid-1970s and very large wildfires in the mid-1990s (both periods of lower annual prescribed burn extents). Fires up to very large sizes are most likely to occur in the 2000s (period of larger prescribe burn extents) and very large fires most likely to occur in the 1980s (higher prescribed burn extents) and 2010s (lowest prescribed burn extents since 2000 but similar to higher extents than the peaks in the 1960s and 1980s).

These decadal-scale relationships are visualised in Figure 9, showing the Pearson correlation coefficient between annual prescribed burn extent and probability of large wildfires for time lags of 0–60 years. Except for a two-year period in the LMZ region, the forested regions show no significant reduction in the probability of large wildfires in the decade after prescribed burns. The woodland Perth region shows a reduction for ten years, which is in contradiction to the regression results for the Perth region in Table 3.

All regions show a significant positive correlation generally between 10–25 years and a significant negative correlation at longer timeframes (starting between 30 and 45 years depending on the region).

To explore the relationship between fire history spatial patterns and large wildfires, linear regression models were generated for the mean probability of a large wildfire for each year (derived from the Probability Density Function results) *versus* each of
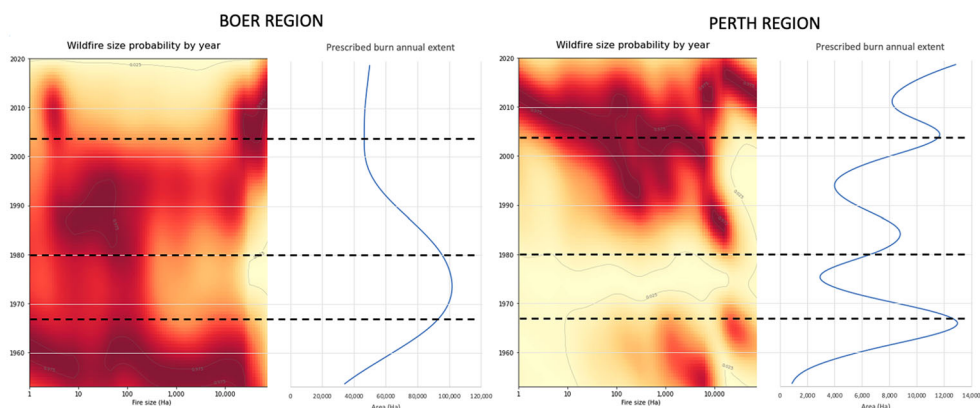
Figure 8. Wildfire size frequency probability distribution for the Boer and Perth regions (left) and GAMs of annual area of prescribed burns (from Figure 5). Red colours indicate higher probability and yellow colours lower probability. Contours show median and 5th percentile and 95th percentiles of probability of fire size for given year against long-term average (where there is a statistically significant greater or lesser probability of a fires of the given size for the given year). Dashed lines indicate the periods of different 'fire management' as defined by Boer et al. (2009) as well as the year 2003 (end of the data used by Boer et al. (2009)).
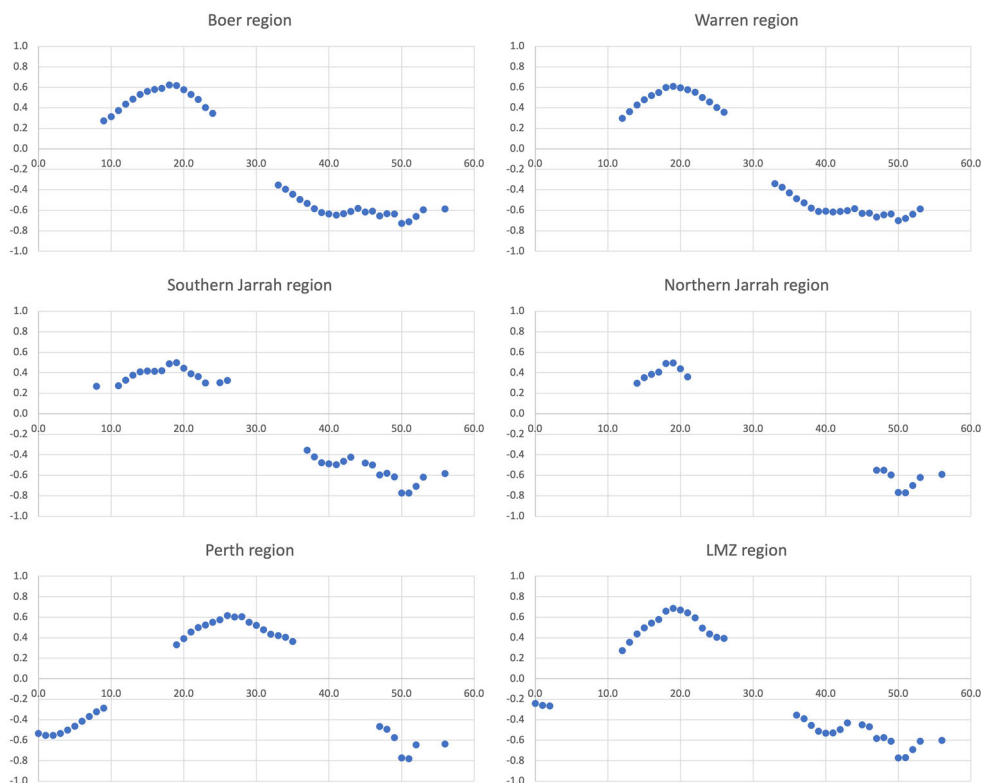
Figure 9. Statistically significant ($p < 0.05$) Pearson Correlation (R) between median probability of large wildfires (>1,000 ha) per year *versus* annual prescribed burn extent for time lags of 0–60 years.

Table 5. Summary of linear regression models Pearson Correlations for annual large wildfire probability versus patch metrics.

S	Boer	Warren	Southern Jarrah	Northern Jarrah	Perth	LMZ
>6TSF PLAND	−0.11	−0.17	**−0.40**	**−0.46**	−0.22	−0.03
>6TSF NP	**−0.49**	0.00	−0.02	**0.82**	**0.68**	**0.29**
>6TSF AREA_MN	**0.38**	−0.11	−0.02	**−0.58**	**−0.47**	**−0.25**
>6TSF PARA_MN	−0.20	−0.02	**−0.44**	**−0.51**	−0.12	−0.09
>6TSF CONNECT	**0.41**	0.20	0.12	**−0.40**	−0.19	−0.08
<=6TSF PLAND	0.11	0.17	**0.40**	**0.46**	0.22	0.03
<=6TSF NP	−0.21	−0.18	**−0.49**	**−0.50**	**0.72**	**−0.21**
<=6TSF AREA_MN	0.06	0.04	**0.33**	**0.43**	**−0.66**	−0.05
<=6TSF PARA_MN	**−0.74**	**−0.64**	**−0.76**	**−0.79**	**0.75**	**−0.52**
<=6TSF CONNECT	−0.19	−0.12	**0.37**	**0.72**	**−0.59**	**0.24**

Numbers in bold indicate statistically significant correlations ($p < 0.05$).

the five patch metrics for areas that were greater than six years' time since fire (>6TSF) and equal to or less than six years' time since fire (<=6TSF) (Table 5).

As with results presented previously in this section, there is no consistent relationship between the probability of large wildfires and the patch metrics. The percentage of area of greater than six years TSF (>6TSF PLAND) was significantly (negatively) correlated with probability of wildfires only for the jarrah regions, indicating that across a significant part of the study area (and in particular the LMZ region as a whole with r = −0.03), the annual area burnt had no significant relationship to the probability of large wildfires. The mean perimeter-area ratio of patches burnt six years ago or less had the mean highest correlation of any patch metric, with significant negative correlations for all forested regions and a significant positive correlation with the woodland Perth region. This indicates that the complexity of fire patches with less time since fire potentially had the largest influence on wildfire probability, with more complex geometries related to lower probability of large wildfires in forest regions.

In most cases, the woodland Perth region had an opposite correlation with time since fire patch geometries than did forest regions. Some of these correlations appear to conflict. The number of patches with less time since fire and number of patches with more time since fire were both positively correlated with the probability of large wildfires and the complexity of patch geometry for areas of less time since fire was also positivity correlated. These apparent contradictions may reflect the dominance of anthropogenic, climatic or other fire regime factors not assessed here.

Discussion

By applying the methodology of Boer et al. (2009) to other regions in the southwest of Australia and including a further additional 17 years of fire history data, we showed that extrapolation of these results to other regions or to a warming and drying climate has little to no statistical validity. Furthermore, we found significant support for the trends measured by Zylstra et al. (2022), in which long-unburned forest was least likely to experience large wildfires. Our results (Figure 9) showed that forest and woodland regions had the strongest and most persistent negative relationship to the likelihood of very large wildfires if less prescribed burning had occurred in the region in the prior 30–45 years.

The Jarrah, Wandoo, Karri and Banksia vegetation complexes of the IBRA sub-regions described in Table 1 have all been classified as different wildfire fuel types (Cruz et al. 2018), with different rates of accumulation and structure (Gould et al. 2011; Tangney et al. 2022). The approximate 0.5 °C increase in average maximum temperature and 30 mm decrease in annual rainfall for the south-west of Australia after the end of the study period used by Boer et al. (2009) has resulted in an altered climate for the region. As a consequence of these spatial and temporal variations, the inapplicability of the findings by Boer et al. (2009) across the region and time period of this study are in line with the discussion in Boer et al. (2009):

> As fuel dynamics, fire behaviour and fire regimes may differ substantially among different forest types, our results obtained for SW Australian eucalypt forests may not hold for forests elsewhere. (p. 141)
>
> … the length of the inhibition period may vary substantially from one environment to another. (p. 140)

On the regional scale of this study, there are several proven factors that influence wildfire likelihood and behaviour in the temperate forests of Australia in addition to the extent of prescribed burning and drought index that form the basis of the wildfire risk management approach in Western Australia. As a result, the fire regime imposed on this region is designed without due consideration of the various factors that are commonly used to effectively define a fire regime.

The current use of the same Dry Eucalypt Forest Fire Model by Cheney et al. (2012) across the southwest region for fuel and fire behaviour (Howard et al. 2020) is highly unlikely to be an accurate representation of either of these fire influences on a broad scale due to the range of biogeographical regions the area covers (such as the predominantly Banksia woodlands of the Perth region) or on a finer scale due to the number of different vegetation complexes present, even within the predominantly open forest regions (Table 1).

An Artificial Intelligence-generated model to predict the probability of large fires across temperate Australia found that while dryness was an important factor, small increases in the proportion of the fire season with a Forest Fire Danger Index (FFDI) of 50 or higher was a significantly more important factor unless dryness was exceptionally high (Clarke et al. 2020). Interestingly the same study found that while biomass (in the form of litter fuel load) was positively correlated with large wildfire probability up to 20 t/ha, above this the correlation stops and then becomes an inverse correlation at litter loads greater than 30 t/ha.

The concept of 'fuel reduction' burning is premised on the assumption that bushfire fuel increases over time. The main component of this 'fuel load' is the leaf litter, however, the only manipulative experiment to date has shown that this has no relationship to rates of fire spread (Burrows 1999). The assumption of increasing litter loads over time is not always a reliable estimate either, as time since fire for fauna to return to a region can have a large impact on the amount, structure or condition of the litter load (Foster et al. 2020). In the Jarrah Forest region in particular, the presence of digging mammals was associated with an almost 50% reduction in surface and leaf litter (Hayward et al. 2016; Ryan et al. 2020).

The main fuel influencing fire behaviour is the understorey of shrubs and tree saplings. This is the primary determinant of flame height (Cheney et al. 2012; Zylstra et al. 2016), as well as crown fire likelihood and rates of spread in all but the lowest intensity fires (Cruz et al. 2021). It has been well documented for our study area that this understorey is promoted by fire, later self-thinning through natural processes of succession (Burrows 1994; McCaw et al. 2002; Bradshaw 2015). This change in structure affects flammability in part by separating the canopy from the foliar biomass, removing 'ladder fuels' in mature (i.e. long undisturbed) forests. These dynamics correlate with a decline in the likelihood of wildfire in long-unburnt, self-thinned forest (Zylstra et al. 2022), and with the findings we have presented here (Figure 9).

Disturbances that contribute to understory growth and higher foliar biomass are not restricted to fires, with regrowth after logging shown to have significant long-term impacts on fuel structure (Wilson et al. 2021), whereas after an initial period of a higher risk fuel structure, disturbance from wildfires had little impact on fuel structures over decadal timescales. These decadal-scale relationships may explain the transition between positive and negative correlations of large wildfire probability and time since fire shown in Figure 9.

Conclusions

The assumption of a direct inverse relationship between annual extent of prescribed burns and wildfires in subsequent years, which underpins wildfire risk management policy Western Australia, has been proven by this study to be inconsistent if not false across the southwest region. There are many factors that influence wildfire behaviour, and therefore wildfire risk management approaches need to account for the complex, multifaceted interactions that contribute to this risk.

With the vast majority of the area burnt by wildfire across the study area being burned by large wildfires, focusing on the temporal changes in the likelihood of large wildfires has yielded some promising results regarding optimising wildfire risk management. In particular, the very strong inverse correlation between probability of wildfires and the spatial complexity of recent fire history across the forested regions of southwest Australia, independent of the average or total size of recent fires (Table 5), indicates that a more complex, nuanced fire history pattern may well yield better wildfire risk management results than the current focus on area and cost-per-area objectives reported annually (DBCA 2021c).

A more spatially complex fire history will also provide better outcomes for biodiversity conservation, with a wide range of fire histories spanning many decades required to provide suitable habitat for the wide range of species present in this highly biodiverse region (Bradshaw et al. 2018). Recent research by DBCA supports this biodiversity benefit (Burrows et al. 2021). Given the traditional Indigenous focus on small-scale rather than broad-scale burns (Lullfitz et al. 2021), our findings underpin the more than 50,000 years of traditional fire knowledge of the Noongar people in the region. This would further benefit biodiversity conservation (and potentially recovery) from the proven maximising of biodiversity values arising from their traditional practices (Lullfitz et al. 2021).

ORCID

Tristan Campbell ⓘ http://orcid.org/0000-0002-3796-9582
S. Don Bradshaw ⓘ http://orcid.org/0000-0001-9068-4060
Kingsley W. Dixon ⓘ http://orcid.org/0000-0001-5989-2929
Philip Zylstra ⓘ http://orcid.org/0000-0002-6946-866X

Data availability statement

The data used to support the findings of this study are available from the corresponding author upon request. All raw data used in the spatial and statistical analyses are available from the public repositories cited in this manuscript.

Disclosure statement

The authors declared that they have no conflicts of interest to this work.

References

Andrys J, Kala J, Lyons T. 2017. Regional climate projections of mean and extreme climate for the southwest of Western Australia (1970–1999 compared to 2030–2059). Clim Dyn. 48(5–6):1723–1747.

Archibald S, Lehmann CER, Gómez-Dans JL, Bradstock RA. 2013. Defining pyromes and global syndromes of fire regimes. Proc Natl Acad Sci USA. 110(16):6442–6447.

Bardsley DK, Moskwa E, Weber D, Robinson GM, Waschl N, Bardsley AM. 2018. Climate change, bushfire risk, and environmental values: examining a potential risk perception threshold in peri-urban South Australia. Soc Nat Resour. 31(4):424–441.

Bentley PD, Penman TD, Bentley PD, Penman TD. 2017. Is there an inherent conflict in managing fire for people and conservation? Int J Wildland Fire. 26(6):455–468.

Boer MM, Sadler RJ, Wittkuhn RS, McCaw L, Grierson PF. 2009. Long-term impacts of prescribed burning on regional extent and incidence of wildfires—Evidence from 50 years of active fire management in SW Australian forests. For Ecol Manage. 259(1):132–142.

Bradshaw FJ. 2015. Reference material for karri forest silviculture. Perth, Australia: Department of Parks and Wildlife Forest Management Series Report No.: FEM067 [accessed 2022 Jul 14]. https://www.dpaw.wa.gov.au/images/documents/conservation-management/forests/FMP/reference_material_for_karri_silviculture.pdf.

Bradshaw SD, Dixon KW, Lambers H, Cross AT, Bailey J, Hopper SD. 2018. Understanding the long-term impact of prescribed burning in mediterranean-climate biodiversity hotspots, with a focus on south-western Australia. Int J Wildland Fire. 27(10):643. http://www.publish.csiro.au/?paper=WF18067.

Bradstock RA. 2010. A biogeographic model of fire regimes in Australia: current and future implications. Glob Ecol Biogeogr. 19(2):145–158.

Bureau of Meteorology. 2021. Maps, recent, past and average conditions, Bureau of Meteorology [accessed 2021 Feb 8]. http://www.bom.gov.au/climate/maps/.

Burrows N. 1994. Experimental development of a fire management model for Jarrah (Eucalyptus marginata Donn ex Sm.) forest. Australian National University. https://openresearch-repository.anu.edu.au/handle/1885/10037.

Burrows N. 1999. Fire behaviour in jarrah forest fuels: 2. Field experiments. CALMScience. 3: 57–84.

Burrows N, McCaw L. 2013. Prescribed burning in southwestern Australian forests. Front Ecol Environ. 11(s1):e25–e34.

Burrows N, Stephens C, Wills A, Densmore V. 2021. Fire mosaics in south-west Australian forest landscapes. Int J Wildland Fire. 30(12):933–945.

Campbell T, Fearns P. 2022. Spatial and temporal validation of in-situ and satellite weather data for the South West Agricultural Region of Australia. J Meteorol Res. 36(1):175–192.

Cheney NP, Gould JS, McCaw WL, Anderson WR. 2012. Predicting fire behaviour in dry eucalypt forest in southern Australia. For Ecol Manage. 280:120–131.

Clarke H, Penman T, Boer M, Cary GJ, Fontaine JB, Price O, Bradstock R. 2020. The proximal drivers of large fires: a pyrogeographic study. Front Earth Sci. 8(April):1–11.

Cruz MG, Cheney NP, Gould JS, Lachlan Mccaw BW, Kilinc M, Sullivan AL. 2021. An empirical-based model for predicting the forward spread rate of wildfires in eucalypt forests. Int J Wildland Fire. 31(1):81–95.

Cruz MG, Gould JS, Hollis JJ, McCaw WL. 2018. A hierarchical classification of wildland fire fuels for Australian vegetation types. Fire. 1(1):13–39.

DAWE. 2020. Interim Biogeographic Regionalisation for Australia (Subregions - States and Territories) v. 7 (IBRA) [dataset]. http://www.environment.gov.au/fed/catalog/search/resource/details.page?uuid=%7B1273FBE2-F266-4F3F-895D-C1E45D77CAF5%7D.

DBCA. 2021a. DBCA-060: DBCA fire history [dataset]. https://catalogue.data.wa.gov.au/dataset/dbca-fire-history.

DBCA. 2021b. DBCA-059: prescribed burn - land management zones [dataset]. https://catalogue.data.wa.gov.au/dataset/land-management-zones.

DBCA. 2021c. Department of biodiversity, conservation and attractions 2020–21 Annual Report. Perth, Australia. https://www.dbca.wa.gov.au/index.php/publications/annual-report-2020-21.

Driscoll DA, Lindenmayer DB, Bennett AF, Bode M, Bradstock RA, Cary GJ, Clarke MF, Dexter N, Fensham R, Friend G, et al. 2010. Resolving conflicts in fire management using decision theory: asset-protection versus biodiversity conservation. Conserv Lett. 3(4):215–223.

Foster CN, Banks SC, Cary GJ, Johnson CN, Lindenmayer DB, Valentine LE. 2020. Animals as agents in fire regimes. Trends Ecol Evol. 35(4):346–356.

Gould JS, Lachlan McCaw W, Phillip Cheney N. 2011. Quantifying fine fuel dynamics and structure in dry eucalypt forest (Eucalyptus marginata) in Western Australia for fire management. For Ecol Manage. 262(3):531–546.

Hayward MW, Ward-Fear G, L'Hotellier F, Herman K, Kabat AP, Gibbons JP. 2016. Could biodiversity loss have increased Australia's bushfire threat? Anim Conserv. 19(6):490–497.

Howard T, Burrows N, Smith T, Daniel G, McCaw L. 2020. A framework for prioritising prescribed burning on public land in Western Australia. Int J Wildland Fire. 29(5):314–325.

Jenkins ME, Bedward M, Price O, Bradstock RA. 2020. Modelling bushfire fuel hazard using biophysical parameters. Forests. 11(9):925.

Jolly WM, Cochrane MA, Freeborn PH, Holden ZA, Brown TJ, Williamson GJ, Bowman DMJS. 2015. Climate-induced variations in global wildfire danger from 1979 to 2013. Nat Commun. 6(1):1–11.

Jones MW, Abatzoglou JT, Veraverbeke S, Andela N, Lasslop G, Forkel M, Smith AJP, Burton C, Betts RA, van der Werf GR, et al. 2022. Global and regional trends and drivers of fire under climate change. Rev Geophys. 60(3):e2020RG000726.

Krebs P, Pezzatti GB, Mazzoleni S, Talbot LM, Conedera M. 2010. Fire regime: history and definition of a key concept in disturbance ecology. Theory Biosci. 129(1):53–69.

Loehle C. 2004. Applying landscape principles to fire hazard reduction. For Ecol Manage. 198(1–3):261–267.

Lullfitz A, Pettersen C, Reynolds R, Eades A, Dean A, Knapp L, Woods E, Woods T, Eades E, Yorkshire-Selby G, et al. 2021. The Noongar of south-western Australia: a case study of long-term biodiversity conservation in a matrix of old and young landscapes. Biol J Linn Soc. 133(1):432–448.

McCaw WL, Neal JE, Smith RH. 2002. Stand characteristics and fuel accumulation in a sequence of even-aged Karri (Eucalyptus diversicolor) stands in south-west Western Australia. For Ecol Manage. 158(1–3):263–271.

McGarigal K, Cushman SA, Ene E. 2012. FRAGSTATS: spatial pattern analysis program for categorical and continuous maps [software] Ver. 4. http://www.umass.edu/landeco/research/fragstats/fragstats.html.

Myers N, Mittermeier C, Mittermeier R, Fonseca G, Kent J. 2000. Biodiversity hotspots for conservation priorities. Nature. 403(6772):853–858.

OpenStreetMap Contributors. 2021. Planet dump [dataset]. https://planet.osm.org.

Ryan CM, Hobbs RJ, Valentine LE. 2020. Bioturbation by a reintroduced digging mammal reduces fuel loads in an urban reserve. Ecol Appl. 30(2):1–12.

Seabold S, Perktold J. 2010. Statsmodels: econometric and statistical modeling with python. Proceedings of the 9th Python in Science Conference. Austin, Texas.

Serven D, Brummitt C. 2018. pyGAM: generalised additive models in python [software].

Skakun R, Whitman E, Little JM, Parisien MA. 2021. Area burned adjustments to historical wildland fires in Canada. Environ Res Lett. 16(6):064014.

Tangney R, Miller RG, Fontaine JB, Veber WP, Ruthrof KX, Miller BP. 2022. Vegetation structure and fuel dynamics in fire-prone, Mediterranean-type Banksia woodlands. For Ecol Manage. 505:119891.

Virtanen P, Gommers R, Oliphant TE, Haberland M, Reddy T, Cournapeau D, Burovski E, Peterson P, Weckesser W, Bright J, SciPy 1.0 Contributors, et al. 2020. SciPy 1.0: fundamental algorithms for scientific computing in Python [software. Nat Methods. 17(3):261–272.

Wang X, Swystun T, Oliver J, Flannigan MD. 2021. One extreme fire weather event determines the extent and frequency of wildland fires. Environ Res Lett. 16(11):114031.

Wilson N, Bradstock R, Bedward M. 2021. Detecting the effects of logging and wildfire on forest fuel structure using terrestrial laser scanning (TLS). For Ecol Manage. 488:119037.

Zylstra P, Bradstock RA, Bedward M, Penman TD, Doherty MD, Weber RO, Gill AM, Cary GJ. 2016. Biophysical mechanistic modelling quantifies the effects of plant traits on fire severity: species, not surface fuel loads, determine flame dimensions in eucalypt forests. PLoS One. 11(8):e0160715.

Zylstra PJ, Bradshaw SDA, Lindenmayer DB. 2022. Self-thinning forest understoreys reduce wildfire risk, even in a warming climate. Environ Res Lett. 17(4):044022. https://doi.org/10.1088/1748-9326/ac5c10.